ISSN: 2395-1680 (ONLINE)
DOI: 10.21917/ijme.2024.0316

ULTRA COMPACT SEMICIRCULAR SLOT ANTENNA FOR UWB COMMUNICATIONS

Sreejith M. Nair[1] and Manju Abraham[2]
[1]*Department of Electronics, Government College, Chittur, India*
[2]*Department of Electronics, Baseliose Poulose II Catholicose College, India*

Abstract

An ultra compact dipole antenna with a semicircular slot suitable for UWB application is developed and discussed. The developed antenna offers a 2:1 VSWR bandwidth starting from 2.92 GHz to 11.34 GHZ which is wide enough to cover the FCC specified UWB frequency spectrum. This antenna offers an average gain of 5.1 dBi in the entire frequency band with greater than 90% radiation efficiency. Developed antenna has an overall volume of 20.3 × 14 × 1.6 mm3 which is compact when compared with other antennas designs. Another attraction of the proposed structure is the simplicity and less number of dimensional aspects and which makes it a suitable candidate in latest generation communication gadgets.

Keywords:

Open Ended Slot Line, UWB, FCC, Enhanced Gain, Radiation Efficiency

1. INTRODUCTION

Antenna is considered as the most important part of a communication system because it acts as the gateway of that system to entire world. If antenna performance is poor, whatever advanced technology may be the system having, it is of no use. Now a days we are witnessing a drastic change in the communication field that the size of the communication device is reduced and data rate of the same increasing exponentially. This creates a simultaneous challenge and opportunities to an antenna design engineer. The prime task of the researcher is to design and develop a compact antenna having simple structure without compromising the radiation characteristics. The most required characteristics of a high data rate antenna are the increased bandwidth with uniform radiation behaviour. Many designs are already available in the literatures and a nutshell of the same is discussed as follows.

In [1], the UWB characteristic for the structure is attained with the help of a centrally slotted metallic patch whose edges are corrugated, which is very complicated design. A printed monopole for wide band communication access system is presented by Authors in [2]. A large radiation patch based modified circular shaped planar monopole UWB antenna is presented in [3]. A wideband radiator suitable for Wearable Body Area Network is presented in [4] but they are not suitable for normal communications. A planar rectangular monopole UWB radiator with very low gain is presented in [5]. An UWB antenna based on meta-material of miniaturized geometries is presented in [6] but in these antennas, radiation patterns are non uniform in the band of operation. In [7], a four element planar UWB array with a complicated structure is discussed. Novel design of a planar UWB antenna with enhanced gain is presented in [8] but the size of the antenna is very high, so that it cannot be integrated with compact communication modules. A ground-independent planar UWB antenna design is discussed in [9]. In [10], authors introduce a modified edge elliptical antenna with UWB characteristics. A notched microstrip line fed UWB structure design is discussed by L Guo and others in [11]. A planar UWB antenna for on-body communication application is presented in [12]. In [13] a high isolation planar UWB antenna for MIMO based wireless application is discussed. A compact UWB monopole antenna with circular plate is given by the Authors in [14]. A UWB monopole suitable for various spectrum sensing applications, which is derived from a hexagon slot, is presented by T Gayathri and others in [15]. UWB antenna with single band-notched characteristic based on rectangular slotted GND plane monopole is discussed in [16]. K. Kumar and others in [17] presents a wide band radiator with a V slot introduced into a trapezoidal shaped patch and with a quasi-curved ground plane. A circular radiator based low-profile planar wideband antenna is presented in [18] in which the radiation characteristics are non-uniform within the band. In [19] dual element based UWB antenna for MIMO applications is developed and discussed which is of with structural complexities. A circular shaped compact planar UWB antenna with reduced radiation efficiency is presented by authors in [20]. A compact V groove UWB antenna with directive properties is discussed in [21].

CPS fed dipole antenna with a semicircular slot suitable for UWB application is developed. The developed antenna is very compact and offers a 2:1 VSWR bandwidth starting from 2.92 GHz to 11.34 GHZ which is wide enough to cover the FCC specified UWB frequency spectrum. This antenna offers an average gain of 5.1 dBi in the entire frequency band with greater than 90% radiation efficiency. From the simulation and experimental studies it is clear that the proposed antenna exhibits moderate gain and stable radiation patterns in the entire frequency band which ensure that the antenna a potential candidate for UWB applications. The time domain analysis of the antenna is also performed and from these results it is found that the proposed antenna is very much suited for the UWB high data rate communication applications.

2. EVOLUTION OF THE ANTENNA

The evolution of the ultra compact UWB antenna and the obtained radiator with structural notations are shown in Fig.1. The antenna is obtained from an Open Ended Slot line (OES) by removing a semicircle of radius R from the top edge of the OES with centre of the semicircle lies in the intersection of middle point of the slot along X axis and upper edge of the OES. The overall dimension of the antenna after the transformation will remain the same as that of the parental OES.

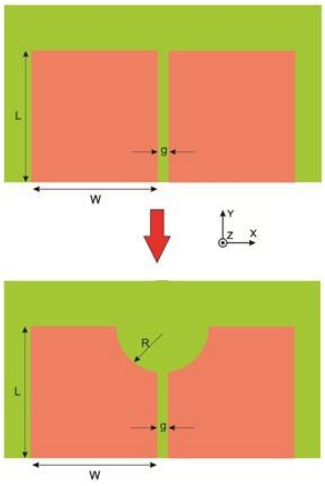

Fig.1. Evolution of Ultra compact semicircular slot UWB from an OES and derived structure with notations

The creation of a new circular slot on the top edge of an OES will change the reflection characteristics of OES. The reflection coefficients of an OES and the OES with a semicircular slot of different dimensions are shown in Fig.2.

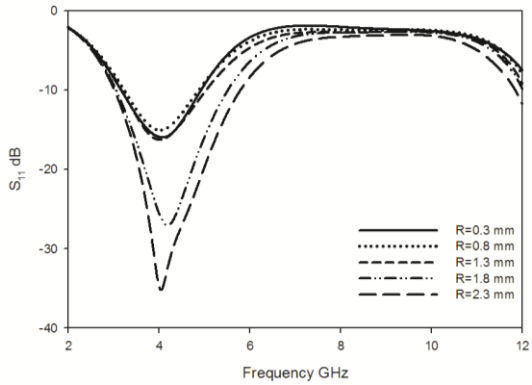

Fig.2. Reflection co efficient of an OES with small R of different dimensions

The figure clarifies that the OES without semicircular slot will acts as a single band dipole with total width approximately equal to half of the wavelength of resonant frequency. The introduction of a semicircular slot at the top edge of the OES will increase the band width. Since the resonance created due to the introduction of semicircular slot with higher radius is asymmetric, there is a possibility of creating an additional resonance near the initial resonant frequency. By properly selecting the parameters this structure can perform like a UWB antenna. The optimization of the antenna is discussed in the parametric analysis session.

3. PARAMETRIC STUDIES

The variation of reflection co-efficient of the antenna with L is shown in Fig.3. According to the figure all the resonances are found to be strongly affected by L. The second and third resonance shows a down shift with L while the first resonance show a very feeble higher shift in frequency with increase in L. This higher shifting of frequency is due to the tendency of fringing field concentration near the slot [22]. The decrease in resonant frequencies of second and third resonance is due to the increase in surface current path length and can be verified from the surface current distribution analysis session. From the variation analysis performed, for the better impedance matching of the structure in the UWB frequency range L of the antenna is optimized as 10 mm.

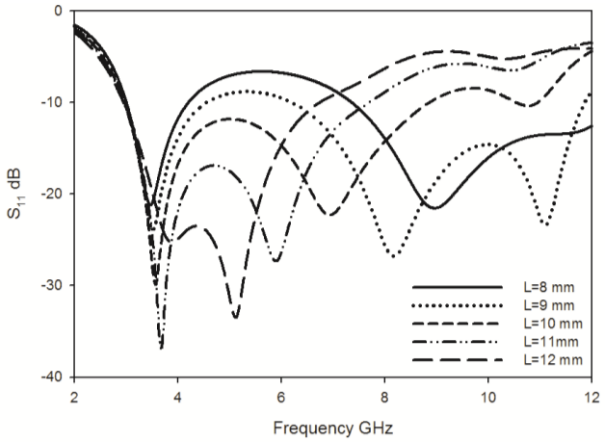

Fig.3. Variation of Reflection co-efficient with L (W=14mm, R=4.38mm, g=0.3mm and h=1.6mm)

The variation of reflection coefficient of the antenna with W is shown in Fig.4. From the figure it is observed that all the three resonances are affected by this parameter. There is a considerable down shift for all the resonant frequencies with W. This is due to the increase in surface current path length of the antenna. The impedance matching of all the curves is found to be good. The W of the antenna is optimized as 14 mm to get the FCC specified impedance bandwidth.

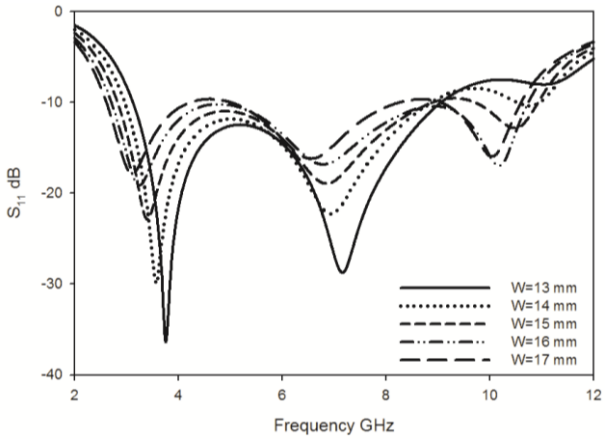

Fig.4. Variation of Reflection co-efficient with W (L=10mm, R=4.38mm, g=0.3mm and h=1.6mm)

The variation of reflection co efficient of the antenna with radius R of the semicircle is shown in Fig.5. For small values of R, the antenna acts as a single band antenna with moderate band width. But for larger values of R, the first and third resonant frequencies show a down shift with increase in R. This is due to the increase in resonant current path length corresponding to these resonances. The second resonant frequency increases with R and is due to the removal of metallic part from the initial current path corresponds to second resonance, which will decrease the current path length.

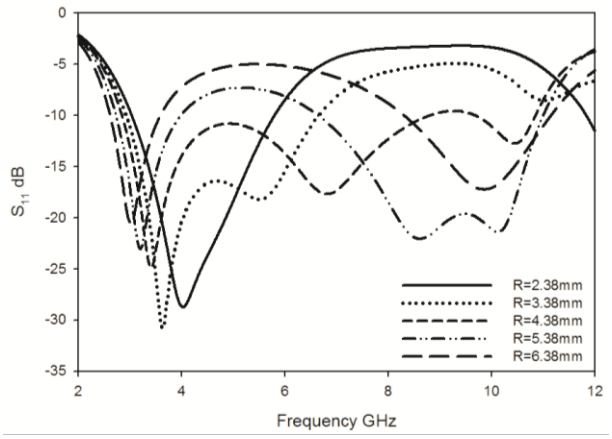

Fig.5. Variation of Reflection co-efficient with R (L=10mm, W=14mm, g=0.3mm and h=1.6mm)

As the final parametric analysis, the effect of substrate height on reflection coefficient is studied. The variation of reflection coefficient of the antenna with substrate height h is shown in Fig.6. From the figure all the resonances are unaffected by the height of the substrate. The matching is slightly affected by the parameter h. This may be due to the variation of input impedance of the antenna with h.

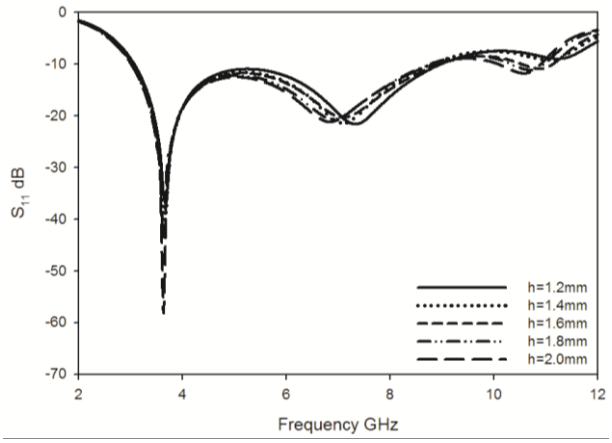

Fig.6. Variation of Reflection co-efficient with h (L=10mm, W=14mm, R=4.38mm and g=0.3mm)

From the parametric analysis of the antenna performed, the design equations of the semicircular slot ultra-wideband antenna are developed and are validated for different substrates with different dielectric constant. The design equations of the antenna are given below.

$$L=0.2\ \lambda_g \quad (1)$$

$$W=0.28\ \lambda_g \quad (2)$$

$$R=0.088\ \lambda_g \quad (3)$$

where λ_g is the guided wavelength corresponding to the first resonant frequency and can be calculated from frees pace wavelength λ_0 as:

$$\lambda_g = \frac{\lambda_0}{\sqrt{\varepsilon_{eff}}} \quad (4)$$

where $\varepsilon_{eff}=(\varepsilon_r+1)/2$ is the effective dielectric constant. To prove the developed design equation, the parameters of the antennas operating in UWB region are computed for different substrates. The substrate parameters of the developed antenna and the dimensional parameters corresponding to each substrate are shown in Table.1.

Table.1. Computed Geometric Parameters of the Antenna with Substrate Description

Laminate	Antenna A	Antenna B	Antenna C	Antenna D
	Rogers 5880	FR4 Epoxy	Rogers RO3006	Rogers 6010LM
h(mm)	1.57	1.6	1.28	0.635
ε_r	2.2	4.4	6.15	10.2
ε_{re}	1.6	2.7	3.575	5.6
g(mm)	0.1	0.3	0.65	0.775
L(mm)	13	10	8.64	6.9
W(mm)	18	14	12.1	9.67
R(mm)	5.68	4.38	3.8	3.04

The simulated reflection co-efficient of the antennas developed using the parameters given in the tables 1 are shown in Fig.7. All the four antennas are ultra wide band in nature and offer sufficient band width with three resonances. The developed design equations are very suitable for developing antennas operating in UWB region in any substrates.

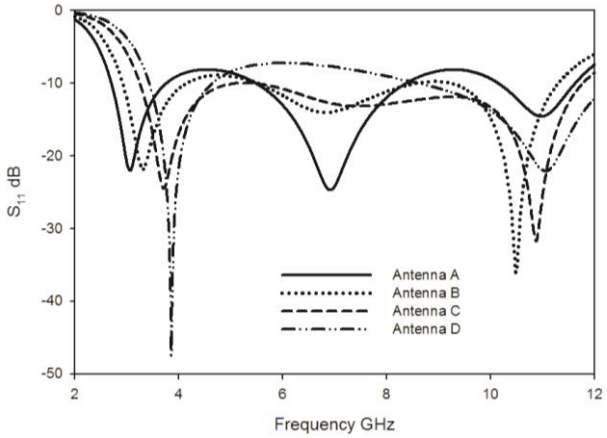

Fig.7. Reflection co-efficient of the Semicircular slot antenna with computed geometric parameters for different substrates

4. RESULTS AND DISCUSSIONS

The simulated and measured reflection co-efficient of the proposed semicircular slot ultra-wideband antenna is shown in Fig.8. The proposed semicircular cut UWB antenna offers a large 2:1 VSWR bandwidth starting from 2.92 GHz to 11.34 GHz. This large bandwidth ensure that the antenna can be used in FCC specified UWB applications. This bandwidth is obtained by merging three resonances centered at 3.67 GHz, 7.2 GHz and 10.85 GHz. From the figure both the curves are in good agreement.

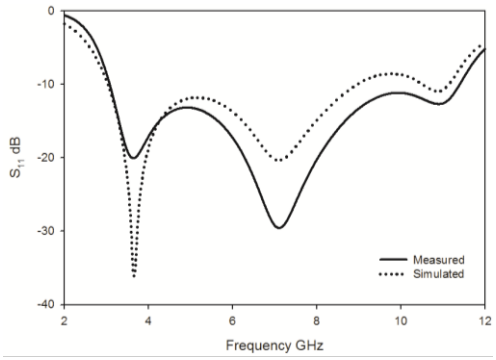

Fig.8. Reflection co-efficient Ultra compact semicircular slot UWB Antenna

The simulated 3D radiation patterns of the semicircular slot UWB antenna at three resonances are shown in Fig.9.

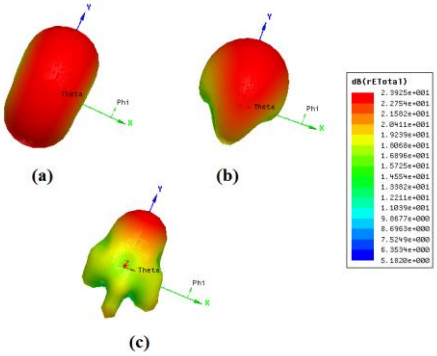

Fig.9. 3D Radiation pattern of the Antenna at (a) 3.67 GHz (b) 7.20 GHz and (c) 10.85 GHz

The radiation pattern of the proposed antenna at 3.67 GHz is shown in Fig.9 (a). The figure shows that the antenna pattern is apple shaped similar to a dipole antenna. There is a small enhancement of power towards the positive Y direction and is due to the inherent directive property of the OES [22]. The null of the pattern is occurred along the X direction.

3D radiation patter of the antenna at second resonance ie at 7.2 GHz is shown in Fig.9 (b). The antenna offers a directive radiation pattern at this frequency with beam maxima pointed towards the positive Y direction. A high amount of back lobe suppression is noticed in this pattern. This effect can be substantiated from the explanation of the surface current pattern of the antenna given in Fig.11 (b). From the current pattern it is found that the current is maximum at the curved edges of the antenna and at all other parts the current is minimum. Thus, the other parts of the radiating structure will acts as a suppressor of backward power. In this pattern also the radiation null lies along the X direction.

The simulated 3D radiation pattern of the antenna at third resonance is shown in Fig.9 (c). At 10.85 GHz the antenna offers a highly directive radiation pattern with a noticeable back radiation suppression. The pattern is slightly distorted with radiation null of the antenna along X axis.

The 2D radiation pattern of the antenna in the two principal planes at different frequencies including the three resonances are given in Fig.10.

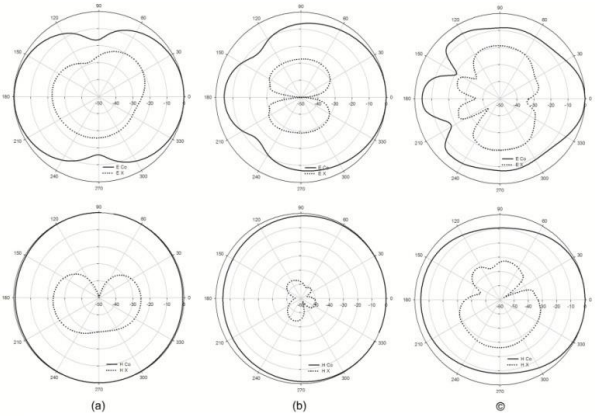

Fig.10. Measured Principal Plane Radiation pattern of the Antenna at (a) 3.67 GHz (b) 7.20 GHz and (c) 10.85 GHz

E and H plane radiation patterns of the antenna at first resonance ie at 3.64 GHz is shown in Fig.10.(a). At first resonance the radiation pattern is omnidirectional like a dipole antenna ie in H plane the pattern is non directional and along E plane it offers a directional radiation pattern with radiation nulls along X axis. The cross polar level at this frequency is found to be in the order of 20 dB in both the planes. The polarization of the antenna remains same as the previous frequency.

The 2D radiation pattern of the antenna at second resonance ie at 7.105 GHz is shown in Fig.10.(b). The antenna exhibits a highly directional behavior at second resonance. The front to back ratio of either plane is found to be better than 5 dB. The cross polar levels along E and H plane are found to be better than 30 dB and 40 dB respectively. The radiation null and polarization of the antenna are along the X direction with radiation maxima occur in the positive Y direction.

Principal plane patterns of the antenna at third resonance 10.85 GHz is shown in Fig.10.(c). From the figure at this frequency also the antenna is directive towards the positive Y direction and the directive property of the antenna increases with frequency. F/B ratio of 7 dB is present in both the planes with a cross polar isolation of 30 dB in E plane and that of 40 dB in H plane. The polarization of the antenna at this frequency also found to be oriented along X direction.

From the 3D and planar radiation pattern analyses, it is evident that the antenna offers a radiation pattern whose beam maxima pointed towards the positive Y direction in the entire operating frequency band. Since the directional property of the antenna is maximum at the second and third resonances, the directive gain of the antenna will be peak at the vicinity of these resonances in the operating band.

Since the beam maxima of the antenna pointed towards the same direction and the polarization of it remains the same orientation it can be concluded that the antenna has very good radiation pattern stability in the entire band of operation.

To explain the radiation mechanism and the reason for resonances, the surface current analysis is very important and unavoidable. Simulated surface current distributions of the antenna at the three resonating frequencies are shown in Fig.11.

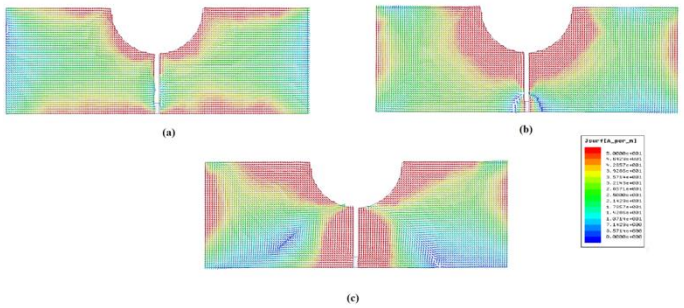

Fig.11. Surface current distribution of the Antenna at (a) 3.67 GHz (b) 7.20 GHz and (c) 10.85 GHz

The surface current distribution of the antenna at first resonance i.e. at 3.67 GHz is shown in Fig.11 (a). The first resonance is created due to the half wavelength long variation of surface current through the entire upper edge length of the antenna. The current is found to be maximum at the centre ie near the slot and is minimum at the edges. This can be also verified from the parametric studies of the parameter W and R. As W increases, the upper edge length increases and result in an increase in current path which will reduce the resonant frequency (Fig.4). Similar variation of first resonant frequency is found in the case of parameter R also. As R increases, the perimeter of the semicircle increases which result in increase in the current path length (Fig.5). As a result resonance gets lowered. Since the current is flowing along the X axis, the polarization of the antenna lies along X direction.

The surface current distribution of the antenna at second resonating frequency 7.2 GHz is shown in Fig.11 (b). Second resonance is due to the surface current variation through the upper edge and upward edges. This can be verified from the parametric analysis. As L and W increases, the lengths of upper and upward edges increases which result in a lower shift in second resonance (Fig.3 and 4). As R increases, a portion from the upper upward edge is removed from the strip, which resulting in a higher shift in resonant frequency (Fig.5).

The surface current distribution of the antenna at third resonance i.e. at 10.85 GHz is shown in Fig.11(c). Here also the surface current shows similar variation as explained in the case of second resonance.

Since the variations in surface current in first and second resonances are found to be in two directions, Electric field analysis is also performed. The simulated electric field plot of the antenna at second resonance is shown in Fig.12 (b). From the field the inference is that the second resonance is a combined effect of electric field variation in both X and Y direction. Thus, the excited mode is a hybrid one. A leaky wave characteristic like a combination of an ordinary wave mode (in X direction) and a slow wave (in Y Direction) is present in both PEC plates of the antenna. This hybrid effect will result in enhanced gain and front to back ratio of the antenna at these frequencies. Since the variation of electric field in Y direction has exactly opposite phase characteristics, they will cancel each other, and the polarization of the antenna remains in X direction. This phase cancellation is the reason for High cross polar purity.

Electric field of the antenna at third resonance is analyzed and given in Fig.12 (c). In Y direction the slow wave shows the same variation while in X direction, the ordinary mode shows a multiple variation. The phase cancellation in both Y directional variation of Electric field will result in a polarization oriented along X direction and a high degree of cross polar purity. Due to the excitation of hybrid mode, the gain and front to back ratio will enhance.

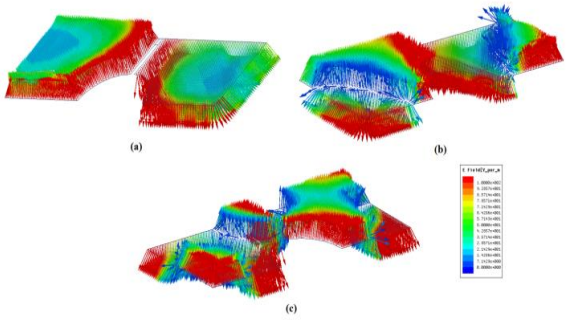

Fig.12. Electric Field distribution of the Antenna at (a) 3.67 GHz (b) 7.20 GHz and (c) 10.85 GHz

Measured directive gain of the antenna as a function of operating frequency and the radiation efficiency of the antenna are given in Fig.13 as solid and dotted lines respectively. The antenna offers an average gain of 4.92 dBi in the entire operating band with a peak gain of 6.9 dBi at higher frequencies. The enhancement in directive gains near the second and third resonance is explained in the previous surface current analysis sessions. The radiation efficiency of the antenna is found to be better than 90% in the entire operating band with an average value of 93 %.

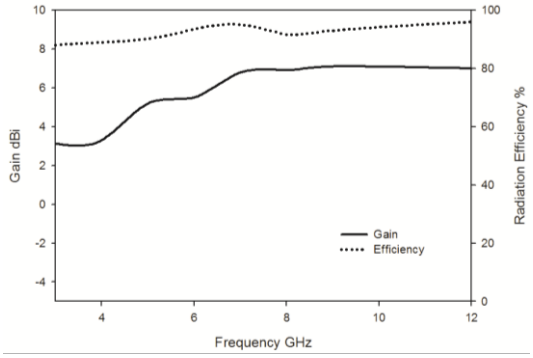

Fig.13. Gain and Efficiency of the Antenna

Since the UWB systems are dealing with extremely narrow pulses, time domain analysis is also equally important for UWB antennas as frequency domain analysis and is unavoidable. Hence, as next step, important time domain parameters of the developed antenna is analysed and result obtained are discussed.

Group delay is defined as the negative derivative of the signal phase with respect to angular frequency. When a signal passes through a device or medium, it experiences both amplitude and phase distortion. A particular wave incident at the input of a device, it may have several frequency components. The group delay gives a measure of average time delay of input signal at each frequency OR it gives a measure of the dispersive nature of the device. To be a good UWB system the group delay must be as small as possible.

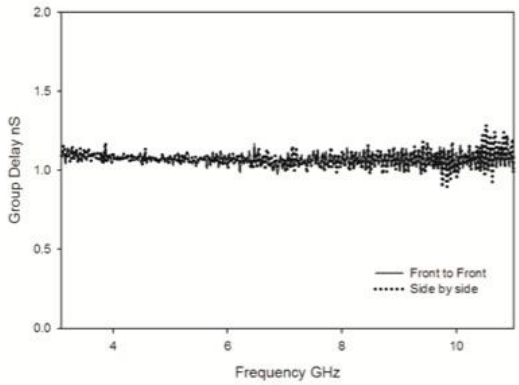

Fig.14. Measured Group Delay of the of the UWB Antennas

The group delay of the developed three UWB antennas as a function of frequency is shown in Fig.14. In the proposed antenna measurements the side by side orientation means the orientations are along bore. From the group delays shown, it is evident that antenna offer a group delays less than 0.5 nS which indicate that the dispersion is very less.

The transfer function of the semicircular slot UWB antenna as a function of φ and θ at the three resonant frequencies are shown in Fig.15. Here also the maximum of the transfer function occurs at bore sight direction where φ and θ equal to 90^0. It is also clear from the figure that the maximum value of transfer function has almost same value in the second and third resonances and at the first resonance it is slightly enhanced. This indicates that there is minimum variation for the transfer function in the range of frequencies formed by the merging of second and third resonances but a slight enhancement in the first resonant frequency range.

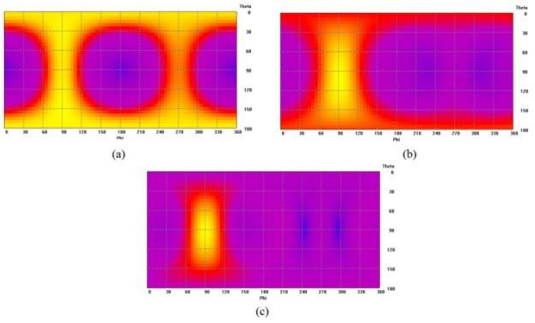

Fig.15. Simulated Transfer function of the UWB Antenna at three resonances in bore sight orientation

The measured transfer function of the UWB antennas in beam maxima direction as a function of frequency is shown in Fig.16. Transfer function is characterized with minimum variation in the frequency ranges.

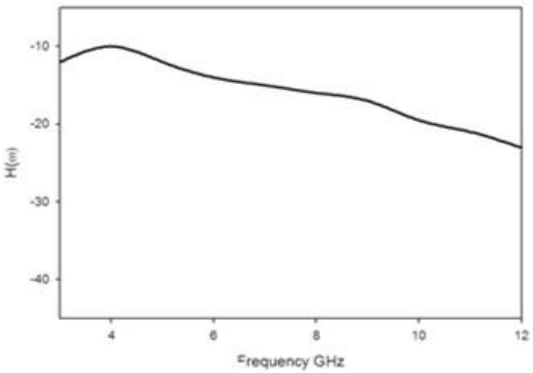

Fig.16.Measured Transfer function of the UWB Antenna at three resonances in bore sight orientation

Impulse response of an antenna system is defined as the response of the system for the impulse signal as input. It is obtained from the transfer function by performing the inverse Fourier transform of it. Calculated impulse response of the proposed UWB antenna along the bore sight direction orientation is shown in Fig.17. And is a good waveform with minimum ringing. There is a small ringing is present in the waveform around 100 nS from the peak value. This may be due to the edge diffraction of signals from antenna.

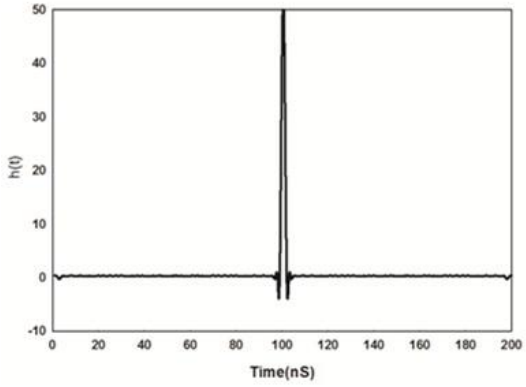

Fig.17. Calculated Impulse response of the UWB Antenna in bore sight orientation

Transmitted and received pulses of the discussed UWB antenna along the bore sight orientation i.e. side by side orientation is shown in Fig.18. From the figure both the received waveforms preserve the shape of the transmitted pulse. The amplitude of the received pulse is less than that of transmitted pulse because of the loss created by the antenna systems and free space loss.

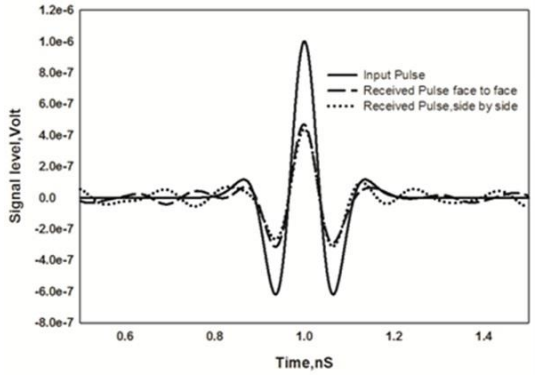

Fig.18.Transmitted and Received pulse of the UWB Antenna in bore sight orientation

Co-relation between the transmitted and received pulses OR fidelity is an important measure of quality of an ultra-wideband antenna system. Fidelity factor of the proposed UWB antennas as a function of azimuth angle are shown in Fig.19. Proposed antenna offers 95 % maximum fidelity. From the fidelity analysis, it is clear that even though the developed antenna is a directional radiator, it preserve the shape of the waveform in all the directions.

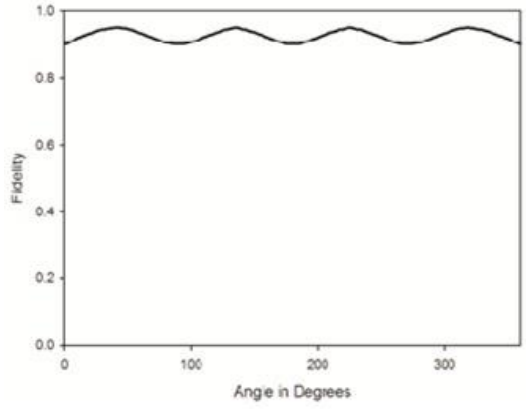

Fig.19. Measured Fidelity factor of the UWB antenna.

EIRP is the amount of power that would have to be emitted by an isotropic antenna to produce the peak power density of the antenna under test. Measured EIRP of all the UWB antenna is shown in Fig.20. From the figure it is found that EIRP of the proposed antenna is with in both the indoor and outdoor masks specified by FCC.

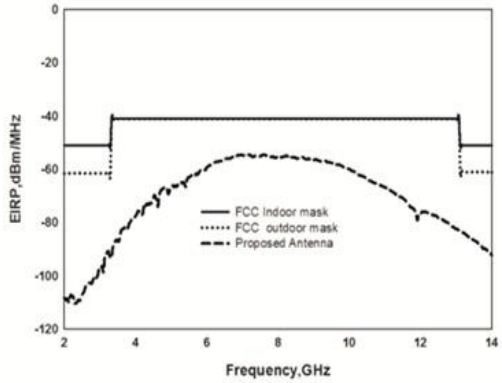

Fig.20. Measured EIRP of the UWB antenna

5. CONCLUSION

CPS fed dipole antenna with a semicircular slot suitable for UWB application is developed. The developed antenna is very compact and offers a 2:1 VSWR bandwidth starting from 2.92 GHz to 11.34 GHZ which is wide enough to cover the FCC specified UWB frequency spectrum. This antenna offers an average gain of 5.1 dBi in the entire frequency band with greater than 90% radiation efficiency. From the simulation and experimental studies, the proposed antenna exhibits moderate gain and stable radiation patterns in the entire frequency band which ensure that the antenna is a potential candidate for UWB applications. The time domain analysis of the antenna is also performed and from these results it is found that the proposed antenna is very much suited for the UWB high data rate communication applications.

REFERENCES

[1] M.C. Ezuma, S. Subedi and J. Pyun, "Design of a Compact UWB Antenna for Multi-Band Wireless Applications", *Proceedings of International Conference on Information Networking*, pp. 456-461, 2015.

[2] P.S. Bakariya and S. Dwari, "A New Compact Planar Ultra-wideband Microstrip Patch Antenna", *Proceedings of International Conference on Advanced Computing and Communication Technologies*, pp. 151-153, 2013.

[3] N. Anveshkumar and A.S. Gandhi, "Design and Performance Analysis of a Modified Circular Planar Monopole UWB Antenna", *Proceedings of International Conference on Computing, Communication and Networking Technologies*, pp. 1-5, 2017.

[4] M. Frank, F. Lurz, M. Kempf, J. Rober, R. Weigel and A. Koelpin, "Miniaturized Ultra-Wideband Antenna Design for Human Implants", *Proceedings of International Symposium on IEEE Radio and Wireless*, 2020, pp. 48-51, 2020.

[5] Xiaodong Deng, Xiaodong Yang, Bingcai Chen and Yu Bai, "A Novel Ultra-Wideband Microstrip Antenna", *Proceedings of International Conference on Cross Strait Quad-Regional Radio Science and Wireless Technology*, pp. 407-410, 2011.

[6] Y. Alnaiemy and N. Lajos, "Design and Analysis of Ultra-Wide Band Antennas based on Metamaterial", *Proceedings of International Symposium on Communication Systems, Networks and Digital Signal Processing*, 2018, pp. 1-6, 2018.

[7] M. Chen and J. Wang, "Planar UWB Antenna Array with Microstrip Feeding Network", *Proceedings of International Conference on Ultra-Wideband*, pp. 1-3, 2010.

[8] E.B. Daher and A. Hoorfar, "Novel Design of a Planar UWB Antenna with Enhanced Gain using a Mixed-Parameter CMA-ES Algorithm", *Proceedings of International Symposium on Radio Science*, pp. 61-61, 2014.

[9] Zhi Ning Chen, T.S.P. See and Xianming Qing, "Small Ground-Independent Planar UWB Antenna",

Proceedings of International Symposium on IEEE Antennas and Propagation Society, pp. 1635-1638, 2006.

[10] A. Mehdipour, K. Mohammadpour-Aghdam and R. Faraji-Dana, "A New Planar Ultra Wideband Antenna for UWB Applications", *Proceedings of International Symposium on IEEE Antennas and Propagation Society*, pp. 5127-5130, 2007.

[11] L. Guo, W. Che and W. Yang, "A Miniaturized Planar Ultra-Wideband Antenna", *Proceedings of* International Symposium on *Antennas and Propagation and USNC/URSI National Radio Science Meeting*, pp. 1053-1054, 2018.

[12] N. Chahat, M. Zhadobov, R. Sauleau and K. Ito, "A Compact Planar UWB Antenna for on-body Communications", *Proceedings of European Conference on Antennas and Propagation*, pp. 3627-3630, 2011.

[13] A.H. Radhi, R. Nilavalan, H.S. Al-Raweshidy and N.A. Aziz, "High Isolation Planar UWB Antennas for Wireless Application", *Proceedings of International Conference on Microwave, Advanced Materials and Processes for RF and THz Applications*, pp. 1-3, 2017.

[14] T. Gayatri, N. Anveshkumar and V.K. Sharma, "A Compact Planar UWB Antenna for Spectrum Sensing in Cognitive Radio", *Proceedings of International Conference on Emerging Trends in Information Technology and Engineering*, pp. 1-5, 2020.

[15] T. Gayatri, G. Srinivasu, M.K. Meshram and V.K. Sharma, "Analysis and Design of a Planar UWB Antenna for Spectrum Sensing in 3.1-10.6GHz", *Proceedings of International Conference on Computing, Communication and Networking Technologies*, pp. 1-6, 2020.

[16] P. Rakluea and J. Nakasuwan, "Planar UWB antenna with Single Band-Notched Characteristic", *Proceedings of International Conference on Control, Automation and Systems*, pp. 1978-1981, 2010.

[17] K. Kumar and N. Gunasekaran, "A New Novel Compact Planar UWB Antenna", *Proceedings of International Conference on Signal Processing, Communication, Computing and Networking Technologies*, pp. 41-45, 2011.

[18] E.G. Lim, "Design and Optimization of a Planar UWB Antenna", *Proceedings of International Symposium on East-West Design and Test*, pp. 1-5, 2013.

[19] Y. Wang, F. Zhu and S. Gao, "Design of Planar Ultra-Wideband Antenna with Polarization Diversity and High Isolation", *Proceedings* of *International Conference on Ubiquitous Wireless Broadband*, pp. 1-3, 2016.

[20] R.K. Tanti, S. Warathe and N. Anveshkumar, "Design of a Circular Planar UWB Antenna and its Higher Cut-off Frequency Enhancement", *Proceedings* of *International Conference on Computing, Communication and Networking Technologies*, pp. 1-6, 2019.

[21] Sreejith M. Nair, Manju Abraham, S. Sindhu and M.S. Nishamol, "Compact Coplanar Strip Fed UWB Antenna with Enhanced Gain" *ICTACT Journal on Microelectronics*, Vol. 8, No. 4, pp. 1437-1441, 2023.

[22] Sreejith M. Nair and P. Mohanan, "Design and Development of Coplanar Strip Fed Planar Antennas", Ph. D Dissertation, Department of Electronics, Cochin University of Science and Technology, pp. 1-335, 2013.